ANTITUMOR ACTIVITY AND SELECTIVITY OF A NANOSTRUCTURED PEROXO POLYOXONIOBATE

Luiz C. A. Oliveira[a]*, Cinthia C. Oliveira[a]**, Samuel M. Breder[a], Klaus Krambrock[a] Poliane Chagas[a], Ana P. Heitmann[a], Estella G. da Mota[a], José B. Gabriel[a], Jadson C. Belchior[a], Leonardo A. De Souza[b], Tiago H. Ferreira[c], Sued E. M. Miranda[c], André L. B. Barros[c], Cynthia L. M. Pereira[a], Vinícius D. N. Bezzon[e], Fábio F. Ferreira[f].

[a] Universidade Federal de Minas Gerais, Departamento de Química, Av. Antônio Carlos 6627, Belo Horizonte-MG, 31270-901, Brazil.

[b] Universidade do Estado do Rio de Janeiro, Instituto de Química, Departamento de Química Geral e Inorgânica, Rua São Francisco Xavier 524, Rio de Janeiro-RJ, 20550-013, Brazil.

[c] Universidade Federal de Minas Gerais, Faculdade de Farmácia, Av. Antônio Carlos 6627, Belo Horizonte-MG, 31270-901, Brazil.

[d] Departamento de Física, Centro de Ciências Exatas, Universidade Federal do Espírito Santo (UFES), Campus Goiabeiras, Vitória - ES, CEP 29075-910, Brazil.

[e] Departamento de Física, Instituto de Ciências Exatas e Biológicas, Universidade Federal de Ouro Preto, Campus Universitário Morro do Cruzeiro, Ouro Preto - MG, CEP 35402-136, Brazil.

[f] Centro de Ciências Naturais e Humanas (CCNH), Universidade Federal do ABC (UFABC), Av. dos Estados 5001, Santo André, SP, 09210-580, Brazil.

Corresponding author phone: +55 31 3409-7550

*lcao@ufmg.br

**cinthia.soares.castro@gmail.com

SUPPORTING INFORMATION

PONb structure (Figure S1a) has five different types of oxygen atoms: five bridging atoms μ_2 – O, two bridging hydroxyls μ_2 – OH, six terminal oxygens η – O, four terminal protonated peroxides η – OOH and two terminal deprotonated peroxides η – OO^- bound to the central atoms Nb(V). The Nb(V) atom in crystal lattices of the PONb monomer has a coordination number from 5 to 7, as observed for other polyoxoniobates types reported in the literature[1–3]. B3LYP/LanL2Dz/6-31G(d,p) (gas phase) optimized geometries of the PONb and MB monomers, and the PONb-MB system are shown in Figure S2.

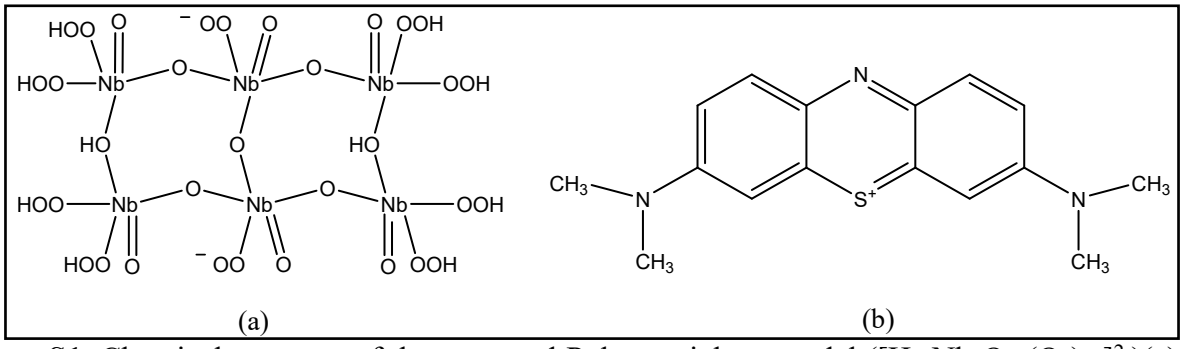

Figure S1. Chemical structure of the proposed Polyoxoniobate model ($[H_{10}Nb_6O_{13}(O_2)_{10}]^{2-}$)(a) and the methylene blue dye (b).

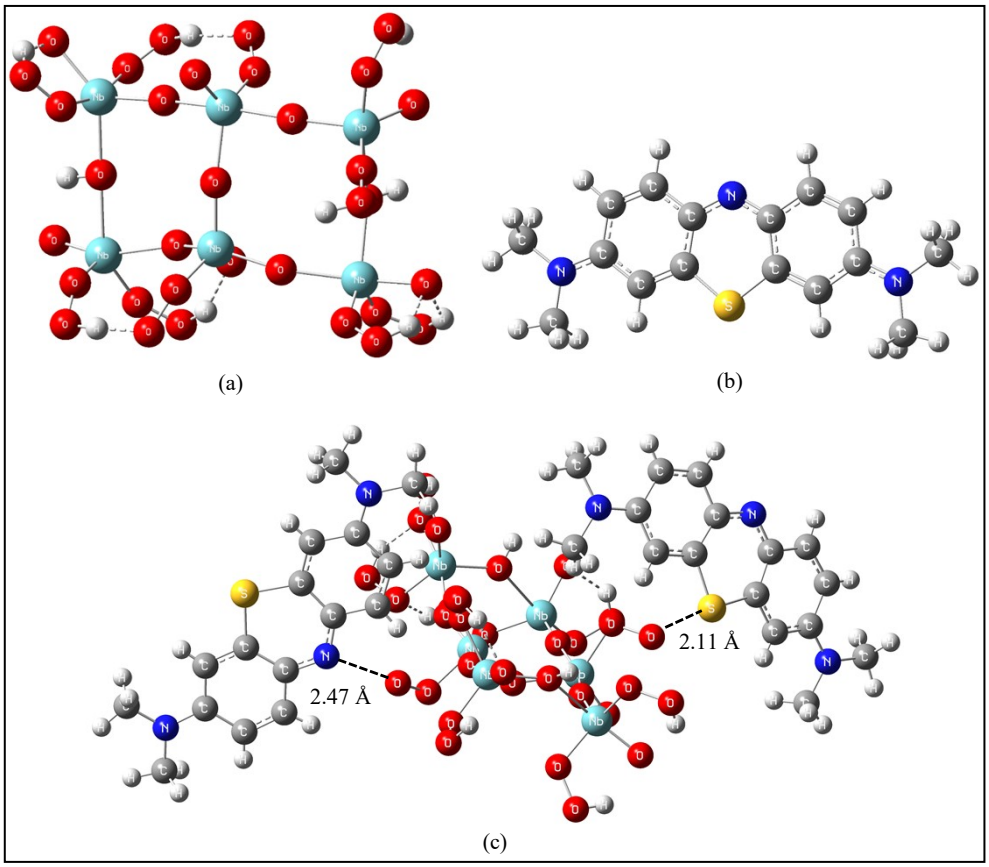

Figure S2. B3LYP/LanL2Dz/6–31G(d,p) fully optimized structures of PONb (a), MB (b) and PONb-MB system (c).

The transitions that contribute the most to the calculated bands (Figures S1b and c) occur between the molecular orbitals highlighted in Table S1. Other contributions (less than 10%) are also present and refer to transitions between innermost molecular orbitals of difficult interpretations. Except for the HOMO-2 orbital (Figure S1d), the LUMO+5 orbital (Figure S3a) is evenly distributed along the PONb surface. This indicates the potential interaction sites that would affect the calculated absorption band at 287 nm (red line in Figure 1b) for the PONb model proposed. The isosurface predominance of the orbitals in the protonated and deprotonated peroxide groups highlights these regions as potential interaction sites of PONb with proton and electron acceptor chemical species, respectively, such as the MB molecule. HOMO orbital (Figure S3b) region located in the heterocyclic ring of MB molecule that interacts through its N atom with PONb monomer may destabilize the

intermolecular interaction. The interaction between PONb and the S atom (heterocyclic ring) of the MB molecule stabilizes the intermolecular interaction in the PONb-MB system (see the circled region in Figure S3b). These results agree with the intermolecular distances calculated at about 2.47 Å (PONb—N-MB) and 2.11 Å (PONb—S-MB), Figure S2c.

Table S1. Transition energy, oscillator force (*f*) and main contributions to the UV-Vis bands calculated at B97D/LanL2Dz/6-31G(d,p) for PONb, MB and PONb-MB system.

Structures	Wavelength / nm	Transition Energy / eV	*f*	Contribution
PONb	287	4.33	0.227	HOMO-2 → LUMO+5 (61%)
MB	216	5.75	0.199	HOMO-2 → LUMO+1 (67%)
	267	4.76	0.763	HOMO-1 → LUMO+1 (49%) HOMO → LUMO+2 (35%)
	524	2.36	0.993	HOMO → LUMO (71%)
PONb-MB	550	2.21	0.739	HOMO → LUMO+3 (60%)

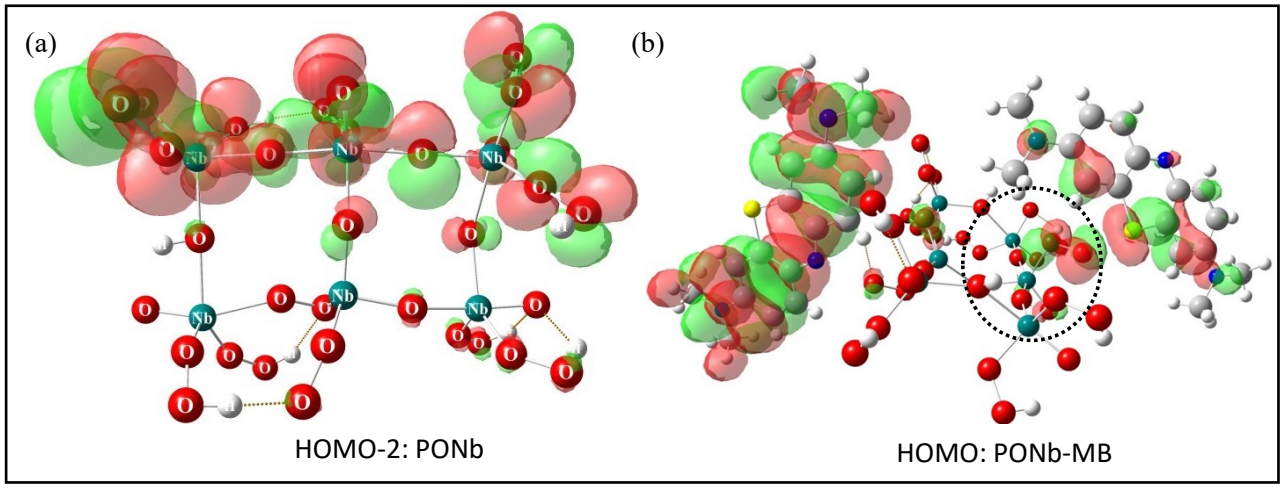

Figure S3. LUMO+5 and HOMO orbitals calculated at B97D/LanL2Dz/6-31G(d,p) (PCM-Water) level for isolated PONb (a) and PONb–MB system (b).

The formation energy of the PONb-MB system, ΔE_F, was calculated as:

$$\Delta E_F = E_{PONb\text{-}MB} - (E_{PONb} + 2E_{MB}) \quad \text{(S1)}$$

In which $E_{PONb\text{-}MB}$, E_{PONb} and E_{MB} correspond to the total energy of the PONb-MB, isolated PONb, and MB fully optimized structures, respectively. The enthalpy (ΔH_F) and Gibbs free energy of formation (ΔG_F) for PONb-MB system were calculated according to Equations S2 and S3, where ΔH_T and TΔS are respectively the thermal correction to enthalpy and entropy contribution evaluated using standard statistical thermodynamic formulae[4]. All calculated parameters are shown in Table S2.

$$\Delta H_F = \Delta E_F + \Delta H_T \qquad \text{(S2)}$$

$$\Delta G_F = \Delta H_F + T\,\Delta S \qquad \text{(S3)}$$

Table S2. Thermodynamic parameters calculated at B3LYP/LanL2Dz/6-31G(d,p) level (p =1 atm, T =298.15 K) for the PONb-MB system. All values in units of kcal mol^{-1}.

Structure	ΔE_F	ΔH_T	$T\,\Delta S$	ΔH_F	ΔG_F
PONb-MB	-55.0	-8.4	-26.3	-63.4	-37.1

Infrared (IR) and Raman spectra (Figure S4) were calculated at B3LYP/LanL2Dz/6-31G(d,p) level for the PONb and MB monomers, and the PONb–MB system. In our harmonic frequency calculations, the influence of possible interactions between PONb–PONb or two PONb–MB systems on band shifts were not considered, since it is a quite demanding computational task. Nevertheless, the main normal modes were assigned and are shown in Table S3. In the IR spectrum of isolated PONb (Figure S4a), we can highlight the following bands: (i) –O–O stretching of η – OOH groups in the range 1200-1350 cm^{-1}; (ii) –Nb–O stretching of η – O groups in the range 750-900 cm^{-1} and (iii) –Nb–OH stretching of μ_2 – OH groups in de 550 cm^{-1} (very low-intensity). In the Raman spectrum for isolated PONb (Figure S4d) are found the low-intensity bands of the –O–O^{-} stretching of the deprotonated peroxide ligands in the region of 1230 cm^{-1}. The formation of the PONb–MB system

slightly shifts the bands relative to the free –O–O^- stretching to the high-energy region of the Raman spectrum. This band shifts from 1230 cm^{-1} (isolated PONb) to about 1250-1300 cm^{-1} (PONb–MB). Simultaneous –O–O^- (PONb) and –C–N / –C–S (MB) stretches are observed in the low-energy region in the range 745-800 cm^{-1} (Table S3) in the IR and Raman spectra. These results indicate that there is an established interaction between the PONb and MB monomers to form a PONb-MB compound.

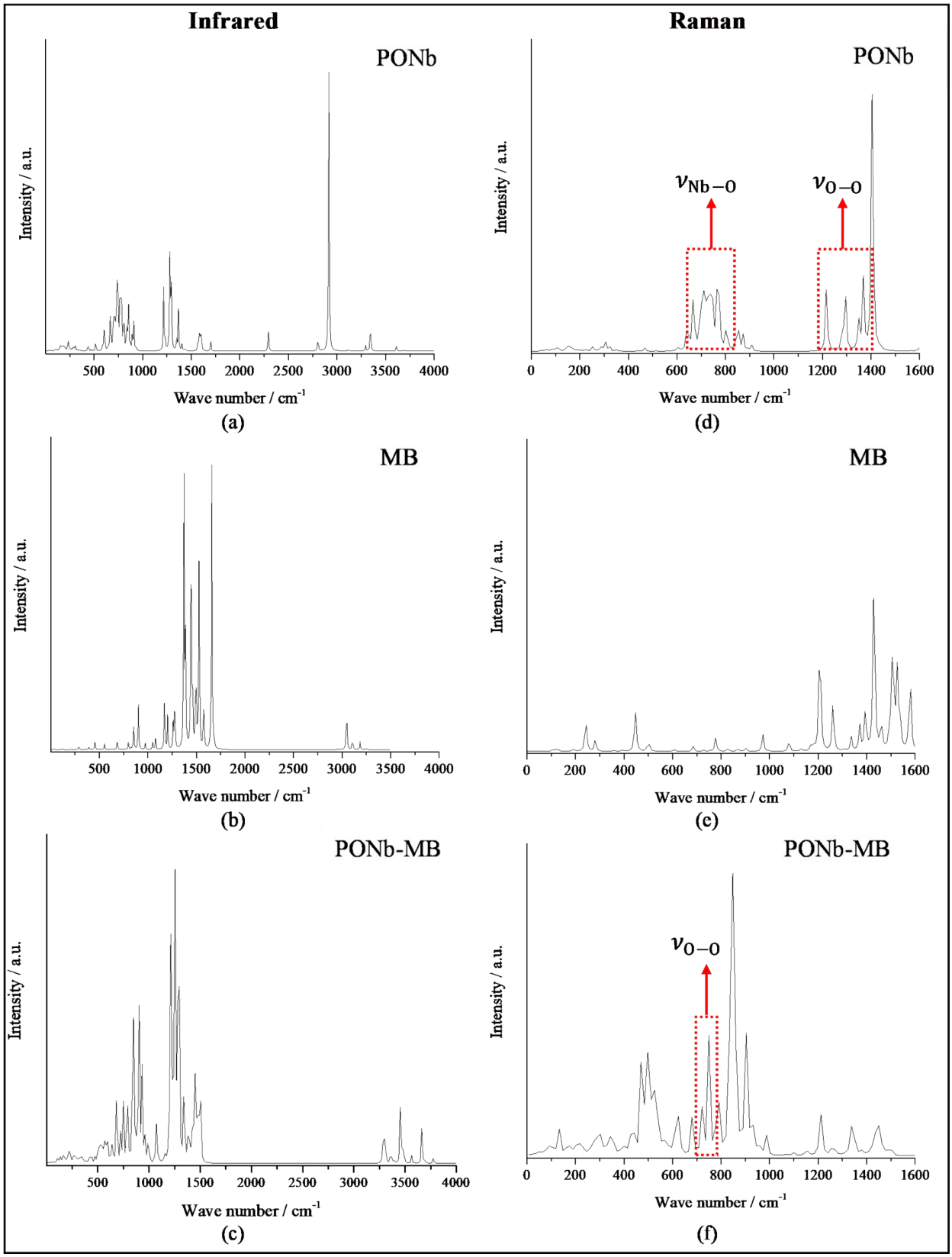

Figure S4. Simulation of the IR and Raman spectra calculated at B3LYP/LanL2Dz/6-31G(d,p) for PONb, MB, and PONb–MB system. The main absorption bands are described in Table S3. In (b) and (f), the highlighted theoretical Raman bands are in good agreement with the experimental results.

Table S3. B3LYP/LanL2Dz/6-31G(d,p) vibrational frequencies (in cm^{-1}) and Raman-IR assignments for PONb, MB, and PONb–MB systems. The assignments of the modes highlighted are in good agreement with experimental results*.

Structures	Vibracional assignments	IV / cm^{-1}	Raman / cm^{-1}
PONb	ν_{O-H}	3900-2750	3200-2900
	ν_{O-O} (protonated peroxides) *	1350-1200	1400-1280*
	ν_{O-O} (deprotonated peroxides) *	-	1230*
	ν_{Nb-O} *	900-750	800-680*
MB	ν_{C-H} (CH_3 group)	-	3250-3000
	ν_{C-C} (aromatic)	1690	-
	ν_{C-N} (heterocycle)	-	1680
	δ_{CH2} (CH_3 group)	1500	-
	ν_{C-C} (heterocycle)	1430	-
PONb-MB	ν_{O-H}	3650-3550	3650-3550
	ν_{C-H} (CH_3 group)	3500-3250	-
	ν_{C-N} (heterocycle)	1270	-
	ν_{O-O} (free protonated peroxides)	-	1300-1250
	ν_{O-O} (deprotonated peroxides) / ν_{C-N} (heterocycle) *	800	770*
	ν_{O-O} (deprotonated peroxides) / ν_{C-S} (heterocycle) *	745	746*

vs: very strong; s: strong; m: medium; w: weak, vw: very weak, ν: stretching; δ: angular deformation.

In the Raman spectrum of the PONb, a peak at 585 cm^{-1} and a broad band around 680 cm^{-1} can be seen, which are usually associated to oxygen-hexacoordinated Nb in a distorted octahedral. In addition, there is an intense and well-defined peak at 878 cm^{-1}, characteristic of Nb-peroxo species formed from the addition of hydrogen peroxide to niobium oxide [5]. The bands related to PONb appear shifted in the Raman spectrum of the PONb-MB material, due to the presence of MB bound to the structure, evidenced in Figure S10. These properties further support the existence of chemical bond between the dye and the niobium complex to form PONb-MB.

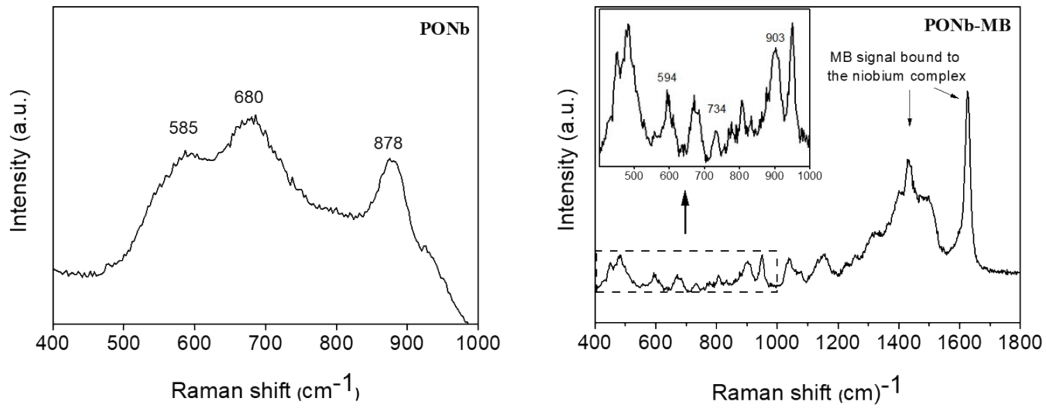

Figure S5: RAMAN spectrum for PONb and PONb-MB.

The structural characterization of the compounds was further investigated by X ray powder diffraction. The main objective here was the comparison of the PONb structure after lyophilization and its precursor, *i.e.*, the precipitated niobium oxyhydroxide[6,7], thus proving that we have a new structure called PONb.

Figure S6a presents the structure functions for lyophilized PONb and Nb_2O_5. There are some differences in PONb S(Q), especially in the regions from 2.2 to 3.0 $Å^{-1}$, 3.0 to 3.2 $Å^{-1}$, and between 4.2 to 8.0 $Å^{-1}$. The Fourier Transform of these results yielded the PDF pattern for the samples, shown in Figure S5b. As can be seen, the main correlations (atomic pair distances) are maintained up to 4 Å for both samples. The PONb G(r) has a higher intensity than the other, which can be related to the higher Hydrogen and Oxygen amount in its structure, yielding a high coordination factor for these atoms in the local structure. Probably, the main local structure where Nb is bonded to O is maintained. Based on the distances calculated up to 10 Å using the Bond_Str software, and based on the Nb_2O_5 CIF file, it is possible to infer some correlations observed in the PDF patterns (S6b). Considering the calculated distances, correlations up to 2 Å can be related to Nb-O pairs; distances between 2 and 3 Å can be O-O, and distances between 3.2 and 4.0 Å can be associated with Nb-Nb nearest neighbor atoms.

It is worth noting that PONb G(r) has higher well-structure correlations further 4 Å, *i.e.*, the correlation peaks have higher intensity as well as well-defined peaks, compared to Nb_2O_5. This can

be associated with a better-organized medium-order structure for this sample, while the Nb_2O_5 preserves most of the local structure (low-order). Therefore, it is possible to infer that the synthesized PONb presents a unique and different crystalline structure than the Nb_2O_5. The PONb linked to MB species generates the PONb-MB structure.

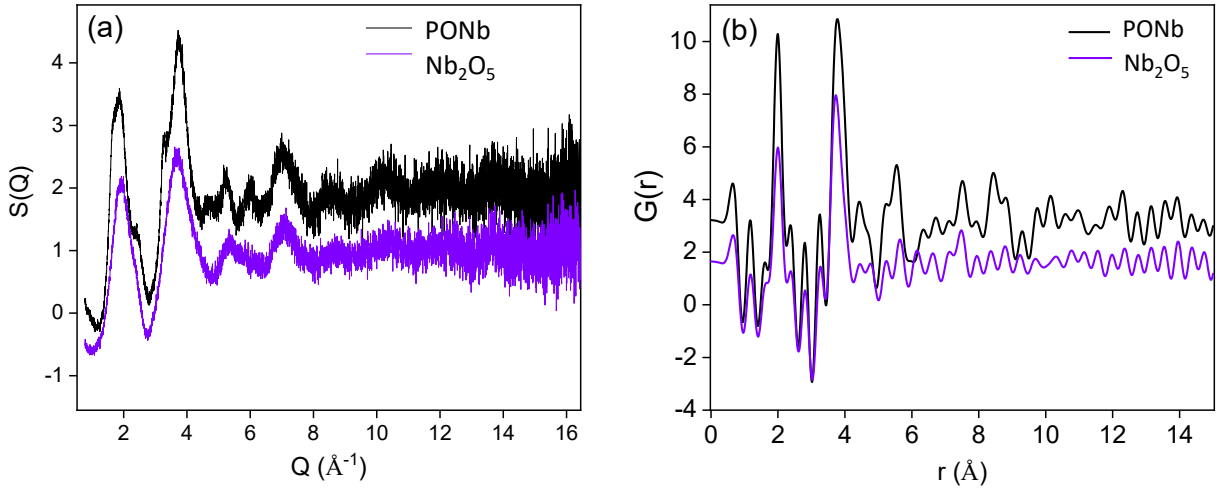

Figure S6. Structure function (a) and PDF patterns (G(r)) for PONb after lyophilization and its precursor, the Nb_2O_5 (b).

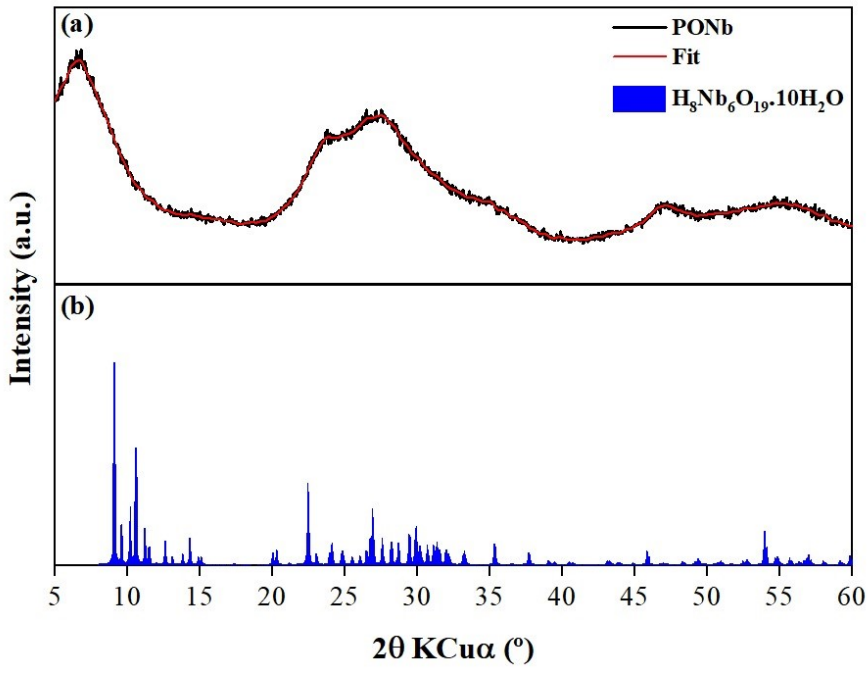

Figure S7. XRD of polyoxoniobate after solvent evaporation (a) and the phase identification using the Powder Diffraction File (PDF) database (JCPDS, International Center for Diffraction Data) (b).

The UV-Vis spectra, shown below, indicate the presence of the compounds even in the presence of the culture media, attesting to their stability.

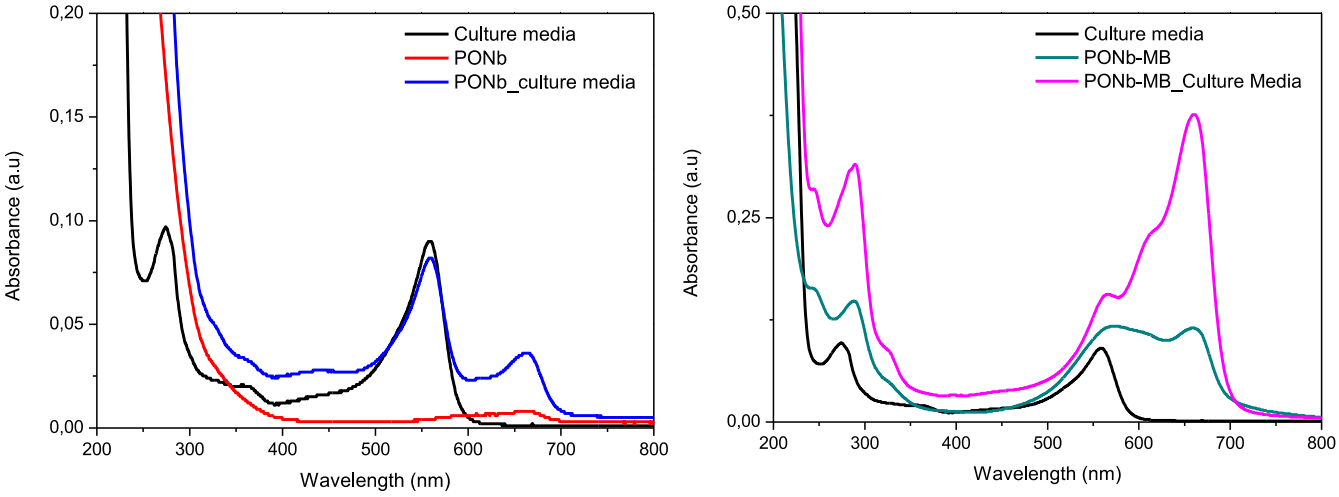

Figure S8. UV-Vis spectra in the presence of the culture media.

The PONb and PONb-MB compounds are organized in clusters. Through DLS (diffuse light scattering) analysis, it was possible to infer the size of these particles. As expected, the results obtained (Figure X) showed that PONb-MB has a larger particle size (660 nm) when compared to PONb (568 nm), since MB is coupled to the structure.

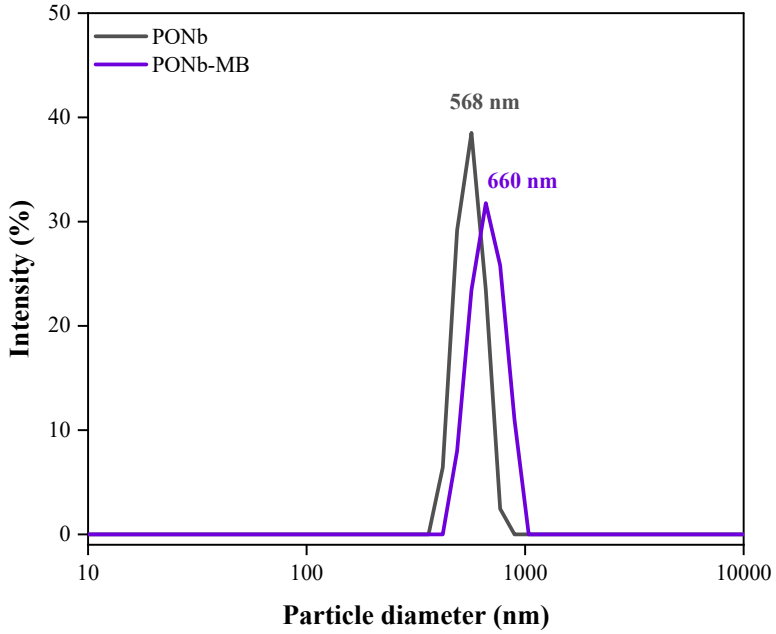

Figure S9: Particle size distribution to PONb band PONb-MB.

REFERENCES

1 J. Geng, Q.; Liu, Q.; Ma, P.; Wang, J.; Niu, *Dalt. Trans*, 2014, **43**, 9843–9846.

2 E.-B. Si, Y.-L.; Wang, *Mol. Phys*, 2009, **107**, 1521–1526.

3 C. Deblonde, G. J. P.; Coelho-Diogo, C.; Chagnes, A.; Cote, G.; Smith, M. E.; Hanna, J. V.; Iuga, D.; Bonhomme, *Inorg. Chem.*, 2016, **55**, 5946–5956.

4 D. A. McQuarrie, *Statistical Thermodynamics*, University Science Books, Mill Valey, 1973.

5 Ziolek, M., Sobczak, I., *Catal. Today,* 2017, **285**, 211–225.

6 H. W. P. Esteves, A.; Oliveira, L.C.A.; Ramalho, T.C.; Gonçalves, M.; Anastácio, A. S.; Carvalho, *Catal. Commun*, 2008, **10**, 330–338.

7 P. Chagas, H. S. Oliveira, R. Mambrini, M. Le Hyaric, M. V. De Almeida and L. C. A. Oliveira, *Appl. Catal. A Gen.*, 2013, **454**, 88–92.